Time-Dependent Behaviour of a Shallow Tunnel in Overconsolidated Clay

Mafalda Lopes Laranjo, Jorge Almeida e Sousa, Paulo Venda Oliveira

Abstract. The presence of groundwater in clayey soils is known to affect its time-dependent behaviour. This paper presents some of the results of a parametric study performed in order to evaluate the influence of the construction technique and the soil/lining relative permeability, in the time-dependent behaviour of a shallow tunnel in overconsolidated clay. The excess pore pressures generated by the excavation are analysed and the evolution of the stress-paths with time around the tunnel section is presented. The movements induced on the soil surface and in depth as well as the loads acting on the support immediately after construction and in long-term conditions are analysed. A circular tunnel excavated at a depth of 20 m was considered and the analysis was performed using a two-dimensional finite-element code that included the MIT-E3 constitutive model.

Keywords: tunnels, overconsolidated clay, MIT-E3, consolidation.

1. Introduction

In clayey soils the changes in total stresses that occur when a shallow tunnel is excavated are immediately reflected not only in changes on the effective stresses but also on the generation of excess pore water pressures. The dissipation of these excess pore water pressures is time dependent and so are the variations on the stress conditions around the tunnel. As a result, the loads acting on the tunnel lining, and the displacements induced on the surrounding soil are also time dependent.

The relevance of this time dependency is associated with the magnitude and the distribution of the excess pore water pressures induced by the excavation and the final equilibrium conditions (Almeida e Sousa, 1998).

The magnitude and the distribution of the excess pore water pressures are largely dependent on the construction method. When using earth balance shields, excess pore pressures are usually positive. This occurs because the applied pressures at the front are greater than the in situ stresses (Yi *et al.*, 1993) and the tail void grouted (Almeida e Sousa, 1998).

In sequential construction methods, such as NATM, in which the excavation is performed allowing for a significant stress relief, the results of numerical analysis (Schmidt, 1989; Mair & Taylor, 1993), of centrifugal models (Mair, 1979) and field observation (New & Bowers, 1994) show that the magnitude and the distribution of the excess pore water pressures are essentially dependent on the stress relief allowed in the front and on the soil type (its history and stress path).

In overconsolidated clays, the reduction of the mean stress and the increase of the shear stress that derive from the excavation, lead to pore water pressures decrease. This decrease will be more significant as the overconsolidation ratio increases and the stress relief on the cutting face rises.

On the other hand, when a normally-consolidated clay is sheared under undrained conditions, pore pressures will increase, contrary to what derives from the reduction of the normal mean stress. In this case, pore pressures will increase or decrease depending on the relative significance of the changes mentioned above. When the stress relief is very significant, the reduction of the mean normal stress near the tunnel section will tend to surpass the increase of the shear stress, and the pore pressures are likely to diminish.

The final equilibrium pore pressures are mainly dependent on the relative permeability between the soil and the support. In fact, if the tunnel is waterproof-type, the dissipation of excess pore pressures will occur in order to re-establish the hydrostatic initial conditions on the ground. On the other hand, if the soil and the support have similar permeability, the tunnel will act as a drain, (Ward & Pender, 1981; Lee & Nam, 2001) and the final pore water pressures will be lower than those initially in situ. This seepage into the tunnel section will continue with the decrease of the water content of the soil and the increase of surface and subsurface settlements (Lopes, 2004).

This paper presents the results of a parametric study concerning the stress paths around the tunnel section immediately after construction and during consolidation, the excess pore pressures generated by the excavation, the deformations induced at the surface and in depth and the loads acting on the tunnel lining.

The analysis was carried out using a two-dimensional finite element code which allows for the consideration of elasto-plastic models with coupled consolidation and includes, among others, the MIT-E3 constitutive model (Venda Oliveira, 2000).

Mafalda Lopes Laranjo, MSc, Escola Superior de Tecnologia e Gestão do IPVC, Portugal, mlopes@estg.ipvc.pt.
Jorge Almeida e Sousa, PhD., Faculdade de Ciências e Tecnologia da Universidade de Coimbra, Portugal, jas@dec.uc.pt.
Paulo Venda Oliveira, PhD., Faculdade de Ciências e Tecnologia da Universidade de Coimbra, Portugal, pjvo@dec.uc.pt.
Submitted on September 29, 2009; Final Acceptance on July 13, 2010; Discussion open until April 29, 2011.

2. The Mit-E3 Model

2.1. General

The MIT-E3 constitutive model results from an evolution of the MIT-E1 and MIT-E2, initially developed at the Massachusetts Institute of Technology to simulate the behaviour of normally consolidated clays. In 1987, Whittle developed the MIT-E3 constitutive model, which enables to accurately reproduce the behaviour of saturated overconsolidated clays (OCR < 8) subjected to cyclic loading (Whittle & Kavvadas, 1994).

The MIT-E3 model links the perfectly hysteretic and bounding surface plasticity formulations together with an elasto-plastic model which describes anisotropic properties of K_0-normally consolidated clays (Whittle, 1993). This model contains a number of assumptions concerning the behaviour of overconsolidated clays, namely:

1. - the overconsolidation ratio (OCR) is not sufficient to accurately describe the behaviour of overconsolidated clays; additional information on the loading history is also required to distinguish between unloading and reloading at a particular overconsolidated stress state;

2. - a load cycle always involves some plastic strains so that there is no purely reversible range of behaviour; the perfectly hysteretic model determines the stiffness and non-linearity of the stress-strain response immediately after a load reversal;

3. - the inclusion of plastic strains, using bounding surface plasticity, provides the means for coupling volumetric and shear behaviour.

2.2. Normally consolidated behaviour

The normally consolidated behaviour is described by a yield surface, a failure criterion, a flow rule and a hardening law. The yield surface, which is initially oriented along the direction of consolidation, has the shape of an ellipsoid (Whittle, 1990) and can be written as:

$$F = -c^2\ p'(2\alpha' - p') + \sum_{i=1}^{5} \left(\{s_i\} - p'\{b_i\}\right)^2 = 0 \qquad (1)$$

where c is the ratio of the semi-axes of the ellipsoid, α controls the size of the yield surface, p' is the mean effective stress, $\{b_i\}$ is a tensor that describes the orientation of the yield surface and $\{s_i\}$ is the deviatoric stress tensor expressed in terms of transformed variables.

The model assumes two hardening rules to describe changes in the size and orientation of the yield surface (Fig. 1). The critical state conditions, describing the behaviour at large shear strains are represented by an anisotropic failure criterion expressed by the equation:

$$h = -k^2\ p'^2 + \sum_{i=1}^{5} \left(\{s_i\} - p'\{\xi_i\}\right)^2 = 0 \qquad (2)$$

where h describes a cone in the generalised stress space with apex at the origin (Fig. 1).

The scalar constant k and the tensor $\{\xi_i\}$ are soil properties which define the size of the cone and the anisotropy of the failure criterion, respectively. The tensor ξ_i is defined by the friction angles in compression (ϕ'_{TC}) and extension (ϕ'_{TE}) at large strain conditions ($\varepsilon_a \approx 10\%$ in undrained shear tests) (Whittle & Kavvadas, 1994).

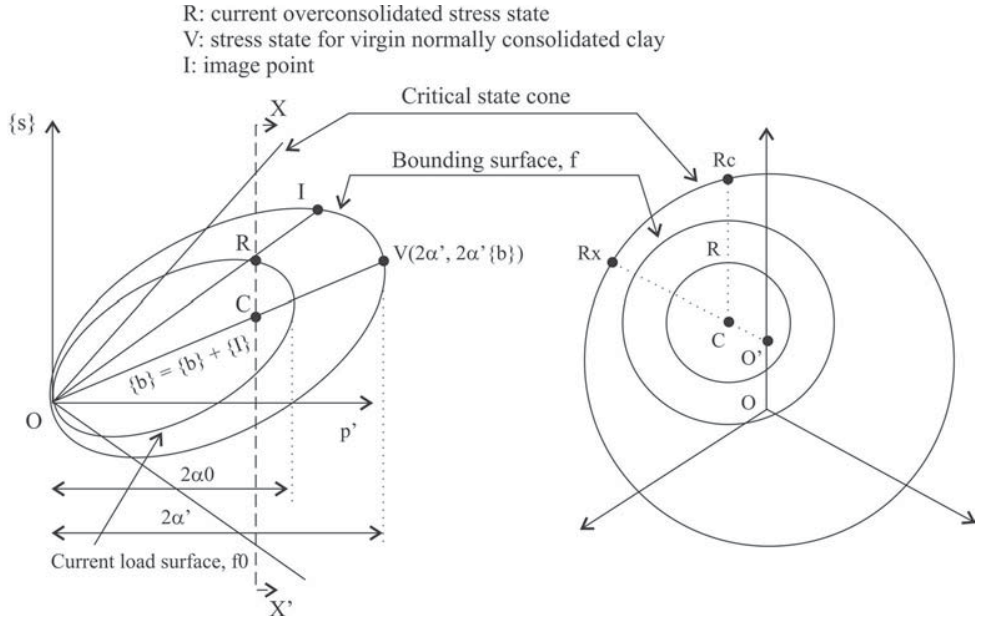

Figure 1 - Yield, failure and loading surfaces for the MIT-E3 model (based on Whittle, 1993).

The model uses a non-associated flow rule in order to describe the critical state failure conditions and K_0 conditions for a one-dimensional compression of virgin normally consolidated clay. Hence, when the stress state approaches the failure cone, there is no volumetric deformation, and in normally consolidated soils in K_0 conditions, any change in the stress state will not change the K_0^{nc} (Ganendra, 1993).

2.3. Overconsolidated behaviour

Laboratory studies on the behaviour of clays show that for unloading/reloading cycles in undrained shear or hydrostatic compression it is possible to observe (Whittle & Kavvadas, 1994):

i) a much stiffer response than the one obtained from the primary loading curve;

ii) a stress-strain hysteretic behaviour;

iii) the existence of plastic strains at the end of each cycle.

To simulate this behaviour of overconsolidated clays, the MIT-E3 model links the perfectly hysteretic model and the bounding plasticity surface. For a load cycle in the stress space, the perfectly hysteretic model describes a closed symmetric hysteresis loop (Fig. 2a), in which the initial stiffness gradually decreases either during the unloading of the virgin consolidation line (from A to B) or during the reloading (from B to A), and that there are no plastic deformations. This model assumes isotropic relations between effective stresses and elastic strain rates, and so there is no coupling between volumetric and shear behaviour.

The MIT-E3 model enables the inclusion of plastic strains in overconsolidated clays (Fig. 2b), providing the means for coupling volumetric and shear behaviour and ensures a smooth transition to normally consolidated behaviour (Whittle, 1993).

In the model, the bounding surface of normally consolidated clay behaviour is described by the yield functions (Eq. (1)), and the plastic behaviour for overconsolidated stress states, R, is linked to the plastic behaviour at the image point *I* (Fig. 1). This situation matches the definition of a load surface f_0 that contains the current (overconsolidated) stress state, homothetic to the bounding surface f with a shape coefficient α_0'/α' (Whittle, 1990).

A detailed description of the MIT-E3 model can be found in Whittle (1993), Ganendra (1993), Whittle & Kavvadas (1994) and Venda Oliveira (2000).

3. Base Problem

3.1. Basic assumptions

The analysed problem consists of a 10 m diameter tunnel excavated at a 20 m depth in an overconsolidated clay (Boston Blue Clay – OCR = 6.0), underlying a superficial 5 m thick layer of sand, as shown in Fig. 3. The groundwater table was assumed to be at the surface and the tunnel lining was simulated by a 0.30 m thick concrete ring, considered in perfect contact with the surrounding soil.

The finite element mesh considered in the numerical analysis, which is shown in Fig. 4, includes 308 quadrangular 8 node elements and 961 nodes. "Hybrid" finite elements were adopted, *i.e.*, the displacements were computed in 8 nodal points (quadratic interpolation) and pore pressures in 4 nodal points (linear interpolation).

At the lateral boundaries of the problem, located on the symmetry axis and 225 m to the right, the horizontal displacements were restrained and in the lower boundary, located 60 m below the ground surface, no displacements were allowed.

In terms of hydraulic boundary conditions, the top and the right boundaries were assumed permeable, while the left and lower boundaries were considered impermeable. The excavation boundary was assumed impermeable. For the sand layer a high permeability coefficient was

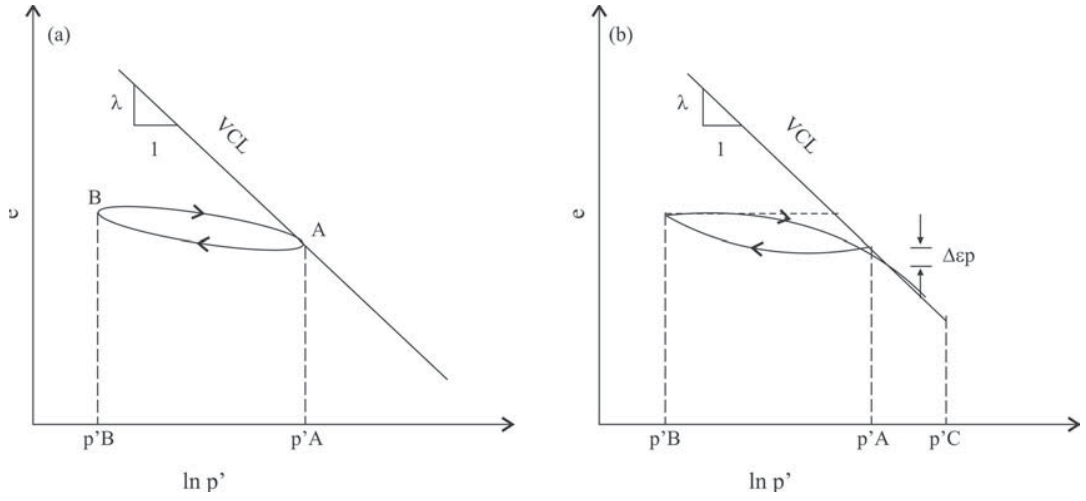

Figure 2 - Conceptual model of unload/reload used by the MIT-E3 model for hydrostatic compression: a) perfect hysteresis; b) Hysteresis and bounding surface plasticity (based on Whittle, 1993).

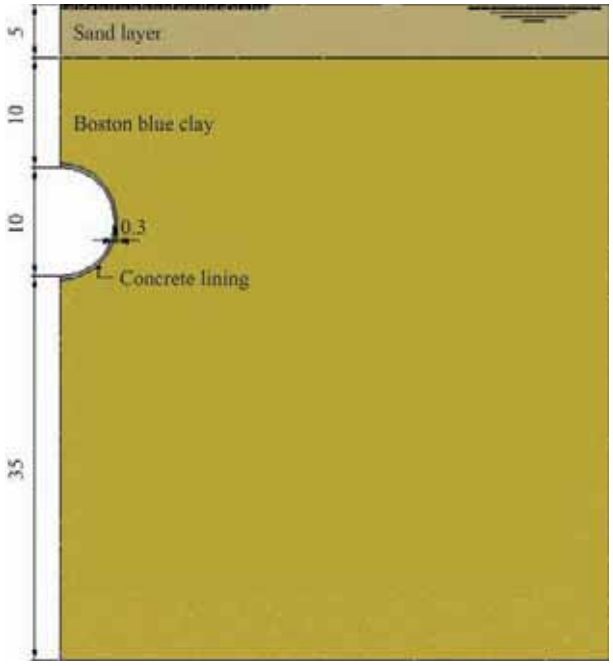

Figure 3 - Geotechnical profile.

adopted and for the clay layer, considered isotropic in terms of permeability, the permeability coefficient adopted was $k = 5 \times 10^{-9}$ m/s.

The ground water pressure was defined by the position of the groundwater table which is considered constant throughout the sand layer.

The geostatic stress state was adopted for the initial conditions and the soil properties shown in Table 1 were assumed.

The behaviour of the sand layer was considered linear, elastic and isotropic, with a Young's modulus (E) of 40 MPa and a Poisson coefficient (ν) of 0.30. For the tunnel lining a linear, elastic and isotropic behaviour was adopted, characterised by E = 30 GPa and ν = 0.2.

Table 1 - Soil properties.

Soil layer	γ (kN/m^3)	K_0
Sand	20	0.5
Boston Blue Clay	20	0.85

The MIT-E3 model, considered for the clay layer, uses 15 input parameters. Some are directly determined from standard laboratory test results: e_0 (initial void ratio); λ (slope of the virgin compression line in e-ln p' space); κ_0 (initial slope of swelling line in e-ln p' space) ; K_0^{nc} ; ν; ϕ'_{TC} ; ϕ'_{TE} . The remaining eight parameters are indirectly obtained from parametric studies: C and n (control the non-linear volumetric swelling behaviour); w (commands the non-linearity at small strains in undrained shear); h (controls the irrecoverable plastic strain); c (controls the undrained shear strength *i.e.* the geometry of bounding surface); S_t (affects the degree of strain softening); γ (regulates the generation of pore pressures induced by shear in overconsolidated clay); ψ_0 (controls the rotation of the bounding surface). The Boston Blue Clay (BBC) parameters are presented in Table 2.

The study was carried out using plane strain conditions, and the convergence confinement method was used to take into account the 3D effects of the excavation (Almeida e Sousa, 1998). In order to simulate soil deformations that occur prior to the installation of the lining, only a fraction (α) of the in situ stresses is relieved. In a second phase, after the installation of the lining, the rest of the equivalent nodal forces are loosened. During these two calculation phases, the behaviour of the soil is assumed undrained and, as a result, excess pore pressures are gener-

Table 2 - MIT-E3 input parameters for Boston Blue Clay (Whittle *et al.*, 1994).

e_0	λ	C	n	h	K_0^{nc}	ν	ϕ'_{TC}	ϕ'_{TE}	c	St	w	γ	κ_0	ψ_0
1.12	0.184	22.0	1.6	0.2	0.48	0.277	33.4°	45.9°	0.86	4.5	0.07	0.5	0.001	100

Figure 4 - Finite element mesh.

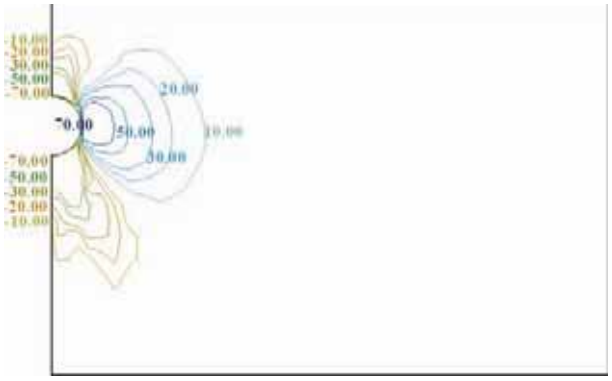

Figure 5 - $\Delta\sigma_y$ immediately after construction (kPa).

ated. For the base problem, a stress relief coefficient $\alpha = 0.63$ was adopted, since it was considered to entail subsidence volumes of approximately 1% of the volume of the excavation on short term conditions (Atwa, 1996; Lopes, 2004), which is in good agreement with the literature (Atwa, 1996; Almeida e Sousa, 1998).

After completion of the construction, the calculations proceeded in order to simulate excess pore pressure dissipation. Several calculation steps were considered, each corresponding to a certain time interval. However, the main purpose of this work is to show clearly the differences between the behaviour immediately after the construction and after consolidation. In this way, the intermediate times of consolidation were not presented in this paper.

3.2. Stress changes

The total stress in the vertical and horizontal direction and shear stress variations immediately after construction are shown respectively in Fig. 5, Fig. 6 and Fig. 7.

The observation of these stress distributions allows identifying five different areas around the tunnel section. Both above and below the tunnel, it is possible to observe a decrease in the vertical stress and an increase in the horizontal stress, which implies a 90° rotation of the principal stress directions. On the other hand, the elements located on the side of the section show an increase in the vertical

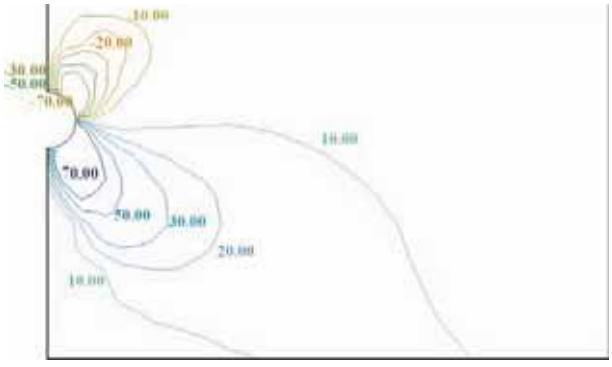

Figure 7 - $\Delta\tau_{xy}$ immediately after construction (kPa).

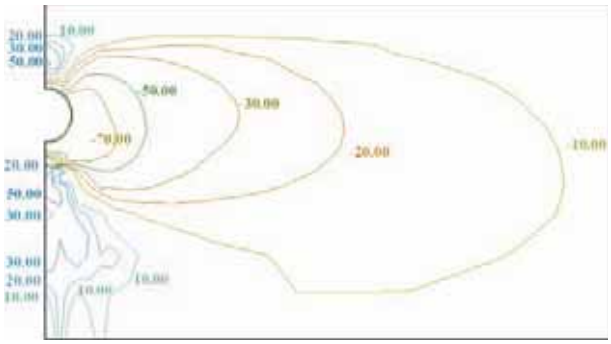

Figure 6 - $\Delta\sigma_x$ immediately after construction (kPa).

stress, due to load transfer, and a decrease in the horizontal stress. At these three locations, as there are no shear stress variations, there is no change in the principal stress directions. The other two areas are located at approximately 45° from the tunnel axis (shoulder and bottom of sidewall). In these areas, the shear stress variation is significant and the principal stress directions are rotated.

As mentioned above, and due to the consideration of undrained conditions, the excavation induces excess pore pressures, as illustrated in Fig. 8. It is possible to observe that in general the excess pore pressures are negative, which is related to the expansion of the cavity, caused by the excavation of the tunnel.

The major negative excess pore pressures were obtained near the invert and the lower part of the sidewall, since these are the locations where the most significant stress variations took place. On the side of the section, negative excess pore pressures are only due to the shear stress variation, hence the negative excess pore pressures are less significant.

After completion of the construction, the calculations proceeded to simulate the consolidation of the clay. During the considered time intervals, excess pore pressures were dissipated in order to establish the final equilibrium conditions. Since the lining was considered impermeable, the final equilibrium was established by the hydrostatic conditions. This situation leads to an increase of the ground water content in the areas where negative excess pore pressures

Figure 8 - Excess pore pressures generated immediately after construction (kPa).

were generated. During consolidation, the variation of the pore pressures will affect the effective stresses around the tunnel, and consequently the ground movements and the loads on the lining.

3.3. Ground movements and lining loads

The surface settlements obtained immediately after construction ($t = 0$) and after consolidation are presented in Fig. 9a. It is possible to observe that the surface settlements tend to decrease with time. Similar conclusion can be drawn from Fig. 9b on what horizontal displacements are concerned. This is due to the expansion of the ground around the tunnel section, induced by the dissipation of the negative excess pore pressures, which is opposite to the vertical and horizontal movements induced by the ground removal.

The ground displacements in depth are presented in Fig. 10. The first observation is that there is significant attenuation of vertical displacements as the distance to the tunnel section increases. In fact, for a final vertical crown settlement (δ_{vc}) of 52.2 mm, the maximum surface settlement (δ_{vs}) was only 4.7 mm, which can be translated by δ_{vs}/δ_{vc} of 0.09.

The consolidation of the clay layer is also responsible for changes in the lining loads. As the effective stresses of the soil decline, the loads acting on the lining rise.

Fig. 11 shows the axial loads acting on the lining immediately after construction ($t = 0$) and after consolidation (t. end), and allows to observe that this load is more significant near the invert and although it tends to increase with time, it does not vary considerably during consolidation.

In terms of the bending moments, Fig. 12 shows that these are practically null after construction and tend to increase with time. In fact, the expansion of the ground around the tunnel section during consolidation is not uniform, hence the bending moment rises.

4. Parametric Study

4.1. General

Table 3 summarizes the calculations carried out during the parametric analysis. The calculations of cases A, B

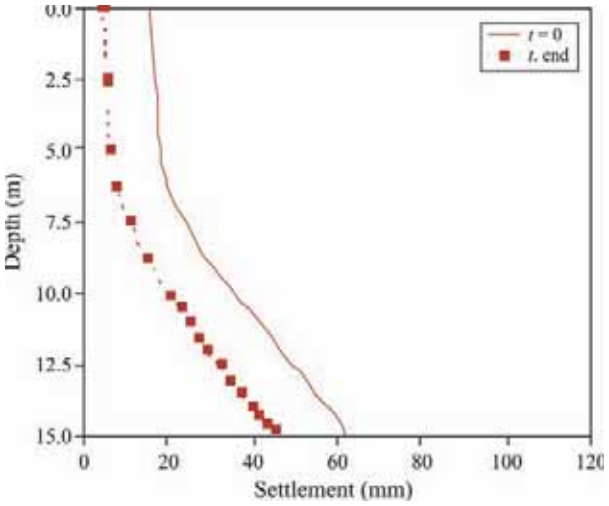

Figure 10 - Ground displacements induced in depth.

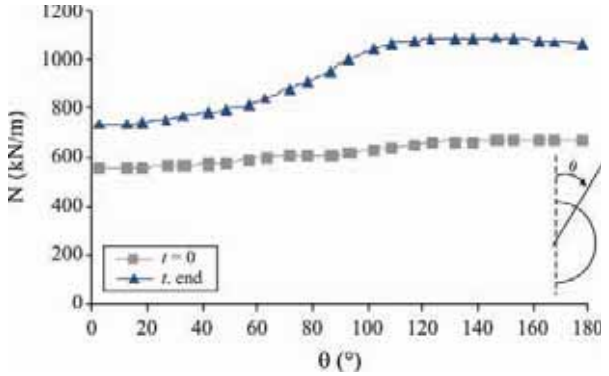

Figure 11 - Axial load on the lining.

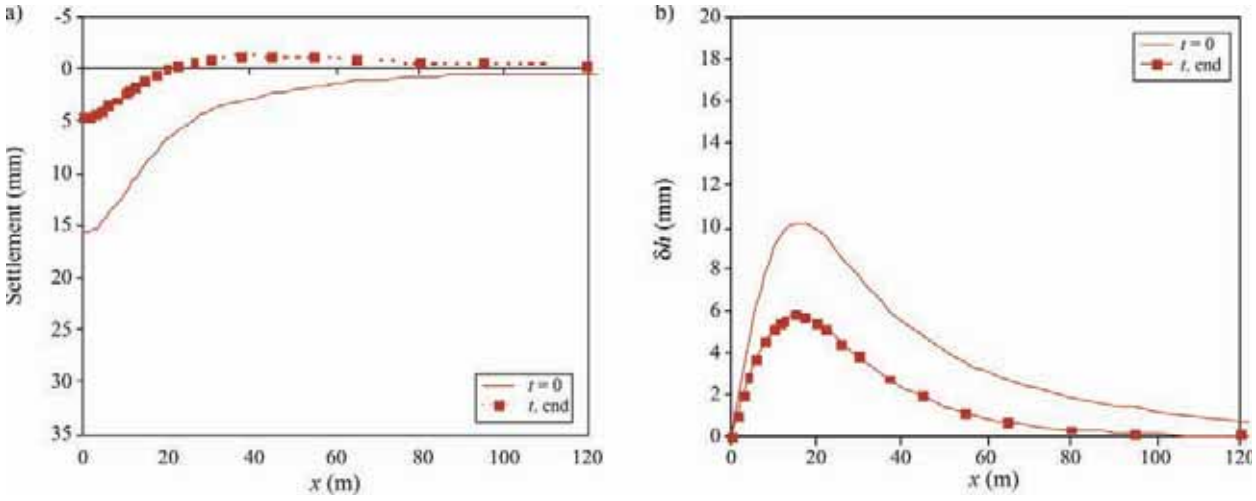

Figure 9 - Displacements induced at the ground surface: a) settlements; b) horizontal displacements.

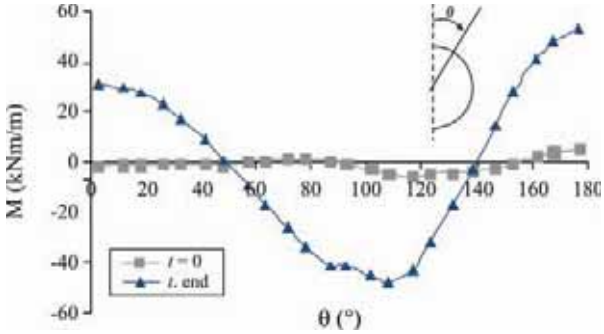

Figure 12 - Bending moment on the lining.

and C were performed in order to evaluate the influence of the construction process on the excess pore pressures. In these cases, the lining was considered impermeable. Case B corresponds to the base problem, which has been presented so far. Cases D, E and F were introduced to clarify the influence of the relative permeability between the soil and the lining, hence the lining was considered permeable and only one relief coefficient was considered.

4.2. Construction process

The analysis of the stress changes induced by the excavation, when considering a larger relief coefficient (case C) in comparison to those illustrated above (case B), suggests the same type of variation during construction, although with longer total stress paths, thus more important variations in both mean and shear stresses.

Fig. 13 shows the pore pressures obtained along the symmetry axis for different relief coefficients immediately after construction. It is possible to observe that the relief of an important part of the equivalent nodal forces prior to the installation of the support (case C), is responsible for larger stress variations on the ground and, consequently, larger negative excess pore pressures. The dissipation of these pore pressures is accompanied by larger displacements in the opposite direction of those induced by the undrained excavation. Numerical analysis performed on the Athens underground show the same behaviour (Drakos *et al.*, 2002).

The ground movements induced by the excavation for cases A, B and C are illustrated in Fig. 14 to Fig. 16. It is

Table 3 - Cases analysed in parametric study.

Case	α	Lining permeability	Soil/lining relative permeability (15 m depth)
A	0.40		
B	0.63	Impermeable	-
C	0.75		
D			1000
E	0.63	Permeable	100
F			10

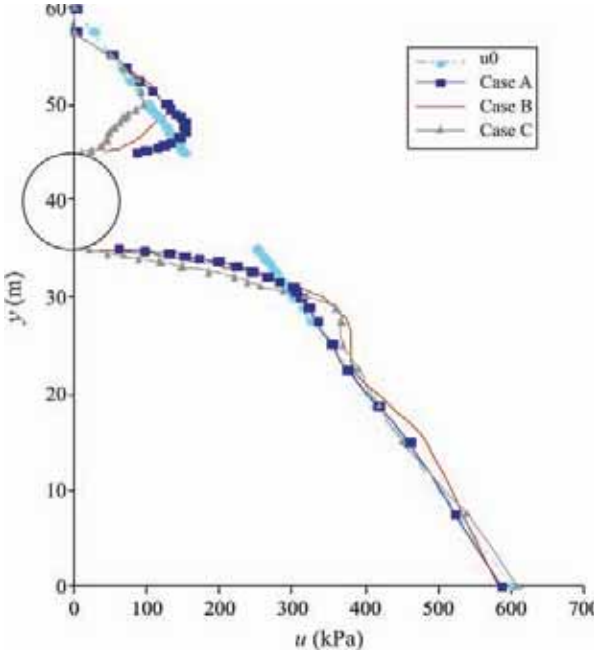

Figure 13 - Pore pressures in the ground along the symmetry axis of the problem, immediately after construction ($t = 0$) with different relief coefficients.

possible to note that the ground movements after construction tend to grow with larger equivalent nodal forces relieved prior to the installation of the support. However, after consolidation, these differences are less significant, since the excavation boundary was assumed impermeable, meaning that the final equilibrium is achieved by the reestablishment of hydrostatic pressures.

The axial loads acting on the lining are presented in Fig. 17 for cases A, B and C, for two time intervals, corresponding to the end of construction ($t = 0$) and the end of consolidation. The results show that the increase of the relief coefficient is responsible for a decrease on the axial load immediately after construction. During consolidation, the pore pressure variation implies an increase of the axial load, which is more significant as the relief coefficient grows. After consolidation the axial load does not significantly differ for the three cases.

The results show a bending moment of approximately zero immediately after construction, which increases with time, especially when the highest relief coefficient is adopted (Fig. 18).

Analysing both axial load and bending moment for cases A, B and C, it is possible to observe that the axial stresses are higher when the relief coefficient is lower, contrary to bending stresses that tend to increase with the increase of the relief coefficient.

Table 4 and Table 5 summarize these conclusions presenting both axial stresses and bending stresses for the three cases, immediately after construction and after consolidation.

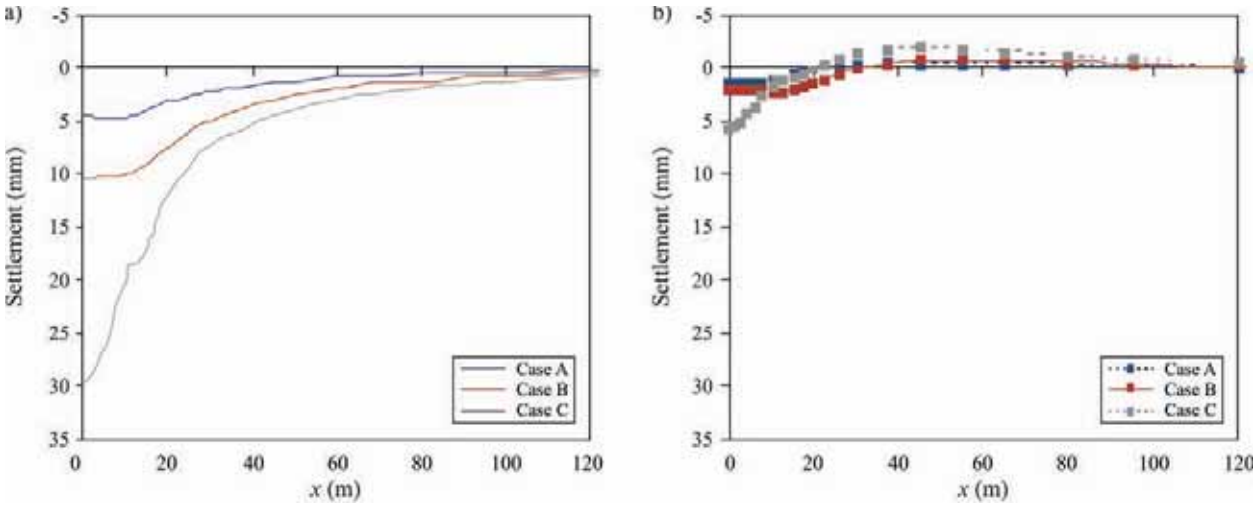

Figure 14 - Ground surface settlements in cases A, B and C: a) immediately after construction; b) after consolidation.

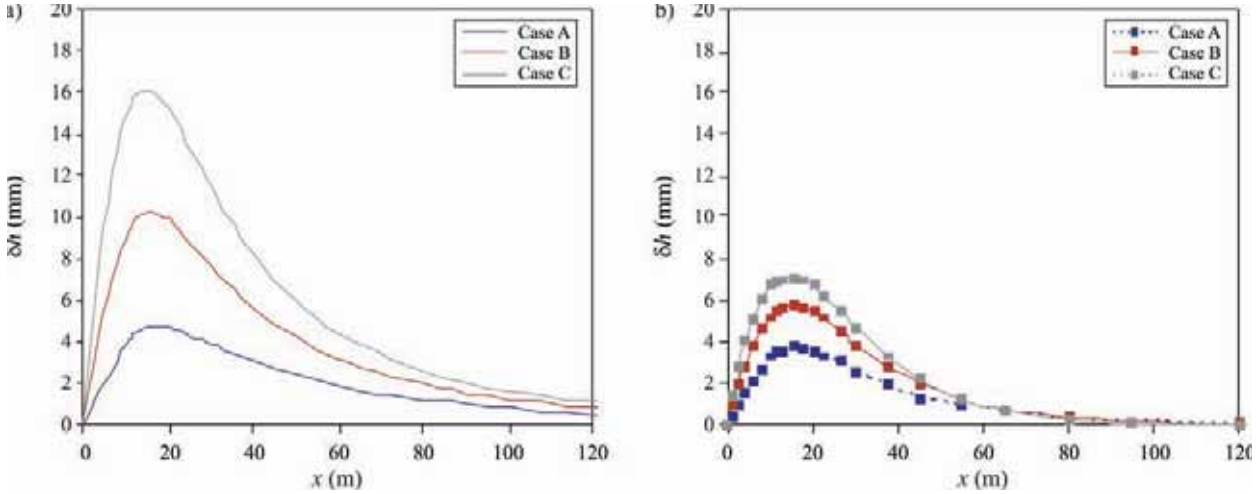

Figure 15 - Surface horizontal displacements in cases A, B and C: a) immediately after construction; b) after consolidation.

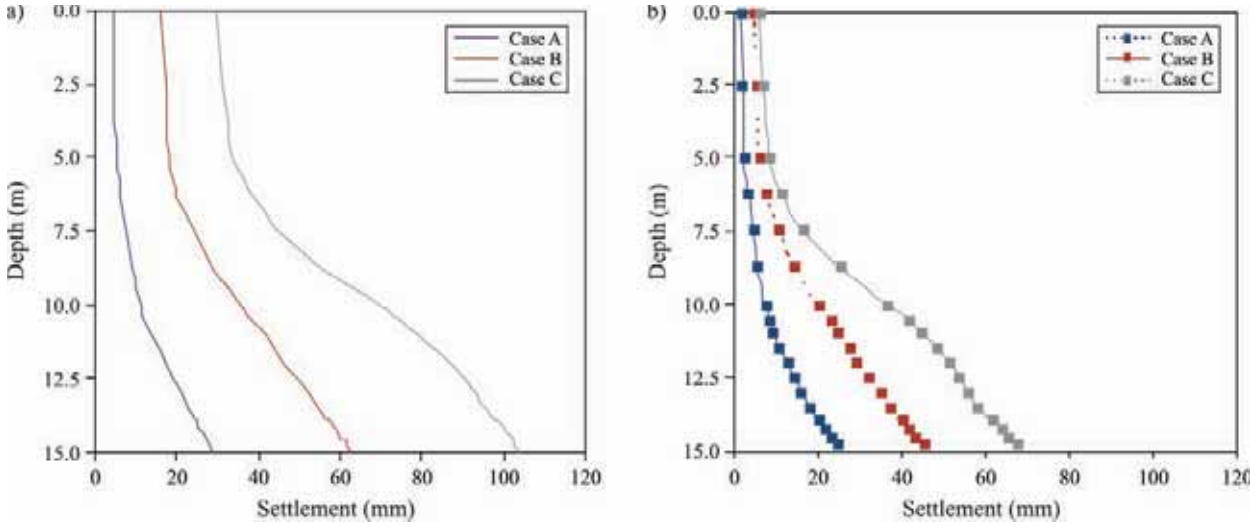

Figure 16 - Ground settlements in depth in cases A, B and C: a) immediately after construction; b) after consolidation.

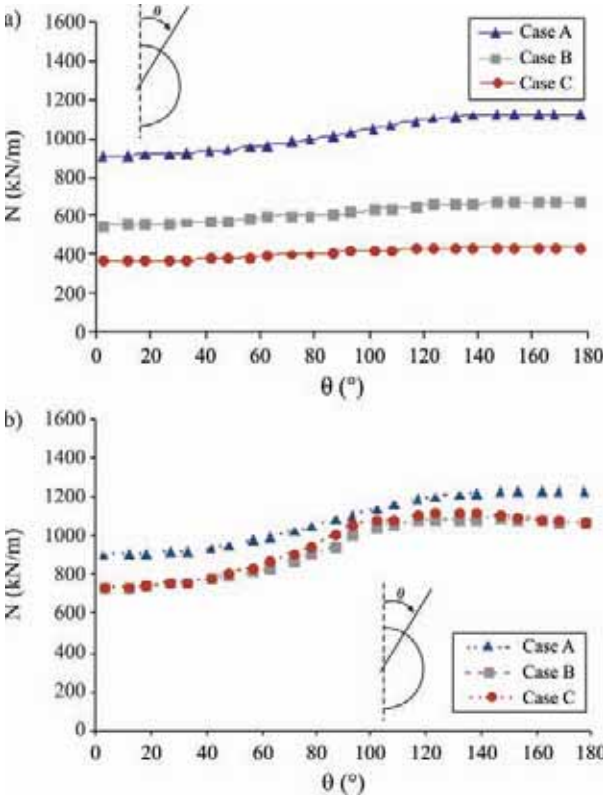

Figure 17 - Axial loads acting on the lining: a) immediately after construction; b) after consolidation.

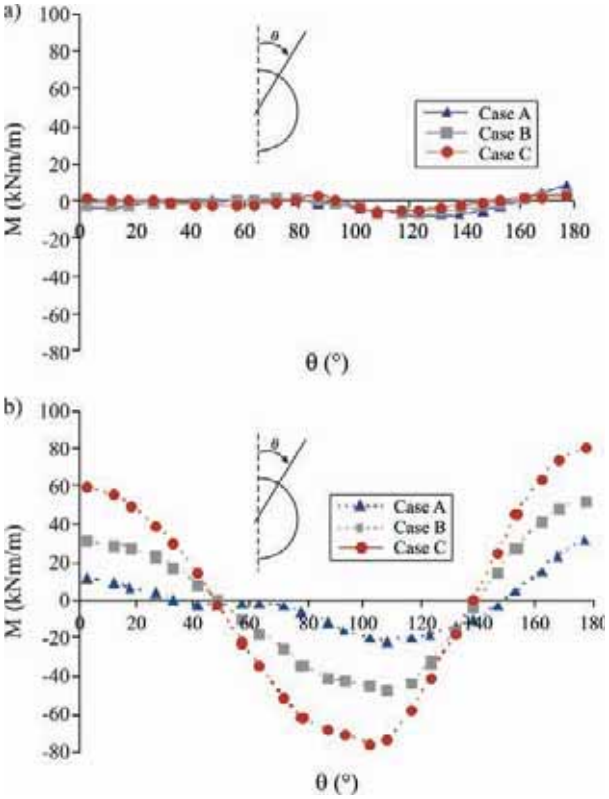

Figure 18 - Bending moments acting on the lining: a) immediately after construction; b) after consolidation.

After construction, the contribution of the axial stresses is more significant than the contribution of the bending stresses, as opposed to what is obtained after consolidation. In fact, when considering a high relief coefficient (case C) the bending stress overcomes the axial stress, thus causing tension in the lining.

4.3. Soil/lining permeability

The effect of the soil/lining relative permeability on the time-dependent behaviour of the tunnel was studied by comparing the results of four different calculations, identified in Table 1 as Cases B, D, E and F. The relief coefficient was assumed $\alpha = 0.63$, as it entails an adequate subsidence

Table 4 - Maximum stresses on the lining immediately after construction.

	$\frac{N}{A}$ (kPa/m)	$\frac{M}{I}$ (kPa/m)	$\sigma = \frac{N}{A} + \frac{M}{I}$ (kPa/m)	% of N	% of M
$\alpha = 0.40$	3750	525	4275	87.7	12.3
$\alpha = 0.63$	2232	328	2560	87.2	12.8
$\alpha = 0.75$	1460	241	1700	85.9	14.1

Table 5 - Maximum stresses on the lining after consolidation.

	$\frac{N}{A}$ (kPa/m)	$\frac{M}{I}$ (kPa/m)	$\sigma = \frac{N}{A} + \frac{M}{I}$ (kPa/m)	% of N	% of M
$\alpha = 0.40$	4086	2140	6226	65.6	34.4
$\alpha = 0.63$	3551	3521	7072	50.2	49.8
$\alpha = 0.75$	3566	5349	8915	40.0	60.0

volume according to the literature. In case B, the lining was considered impermeable, contrary to what was assumed in cases D, E and F, in which the permeability of the lining was considered to be 1000, 100 and 10 times lower that the permeability of the ground, respectively.

In order to simulate a permeable excavation boundary, it was necessary to change the hydraulic boundary conditions of the problem, by altering the permeability coefficient of the finite elements adjacent to the excavation section and by imposing zero pore water pressures on the contact face of these elements and those that materialize the concrete lining, hence allowing seepage into the tunnel.

Since the excavation was performed in undrained conditions, the results obtained for the end of construction are coincident in the four cases and will be referred to as $t = 0$. The obtained differences are significant in the end of consolidation, given that the seepage into the tunnel section provides final equilibrium pore pressures lower than the hydrostatic condition.

Fig. 19 shows the pore pressures along the vertical symmetry axis of the problem for two time intervals (after construction and after consolidation) obtained for cases B and E. The difference between the final and hydrostatic (u_0) pore pressures is more significant for case E, since a drainage-type tunnel was considered.

As the final equilibrium conditions differ, so will the stress-paths and, consequently, the ground movements and the lining loads.

Fig. 20 shows the vertical and horizontal displacements induced in the ground surface for cases B, D, E and F, obtained immediately after construction ($t = 0$) and after consolidation (t. end).

It is possible to observe that both the vertical and horizontal displacements induced on the ground surface when considering a drainage-type tunnel are more significant than those obtained with a waterproof-type tunnel (case B).

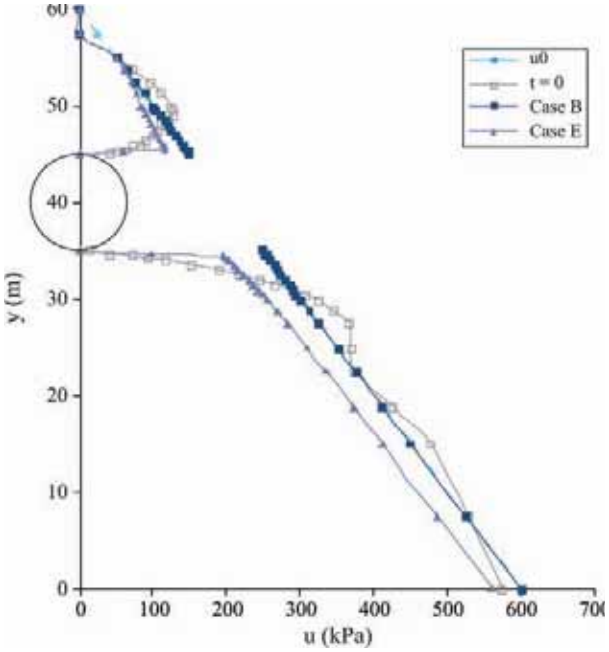

Figure 19 - Pore pressures in the ground along the symmetry axis of the problem, immediately after construction ($t = 0$) and after consolidation (cases B and E).

These differences tend to be amplified with the permeability of the lining, since the global volume of ground surrounding the cavity tends to be reduced as the water flows into the tunnel. In this case, for a soil/lining relative permeability lower than 100, the surface settlements tend to increase during consolidation, contrary to what was obtained with an impermeable lining.

The same behaviour can be observed in Fig. 21, where vertical displacements along the symmetry axis of the problem are illustrated. These results also show an interesting feature regarding the relative vertical displace-

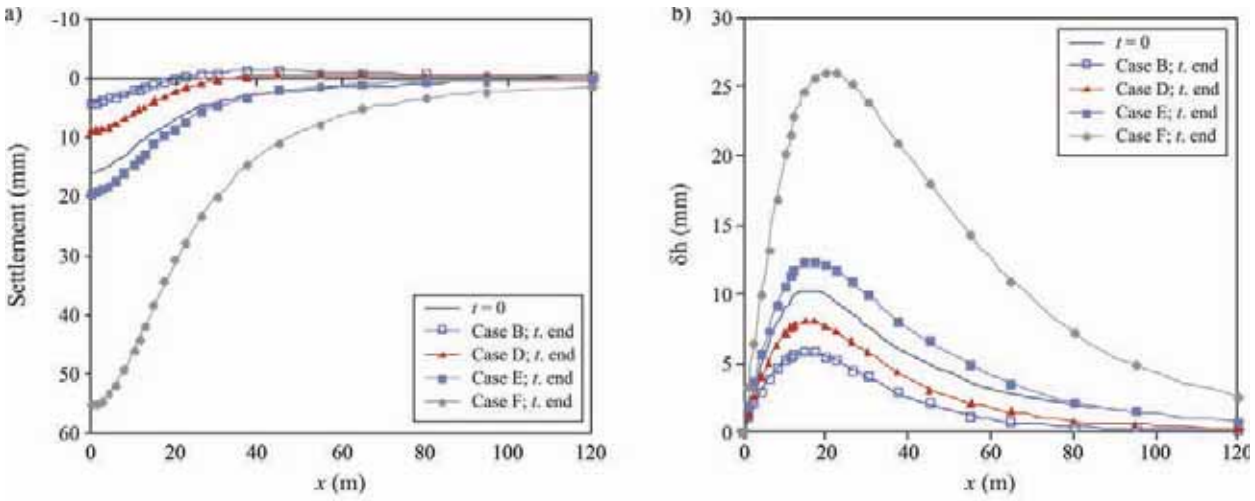

Figure 20 - Displacements induced at the ground surface in cases B, D, E and F: a) settlements; b) horizontal displacements.

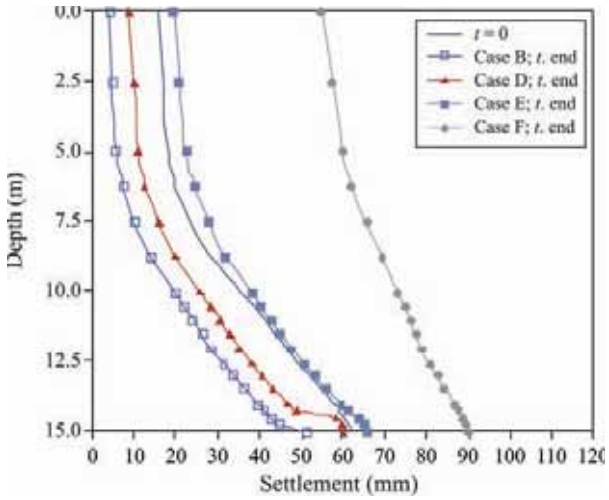

Figure 21 - Ground surface settlements in depth in cases B, D, E and F.

ment between the surface and the tunnel crown (δ_{vs}/δ_{vc}). In fact, as the lining permeability increases, the total head losses in the surrounding ground increase, hence the seepage forces and the effective stresses tend to increase above the tunnel section, causing the approximation of those two points. The ratio (δ_{vs}/δ_{vc}) of these settlements is of approximately 10% for case B (impermeable lining) and 60% for case F.

The axial loads and bending moments on the lining tend to increase during consolidation, more significantly in waterproof-type tunnels, since the water content of the ground in these cases also grows. Fig. 22 demonstrates that an increase of the permeability of the lining will decrease the variation of both axial forces and bending moments during consolidation.

5. Conclusions

In this paper, a numerical study concerning the excavation of a tunnel in clay is presented. The results show that in overconsolidated clay the variations in the normal mean stress and the shear stress induced by the excavation have similar effects on the generation of excess pore pressures. In fact, in overconsolidated clays, due to positive dilatancy, the reduction of the mean stress and the increase of the shear stress, which occur during the excavation, are both responsible for the decrease of pore water pressures. The dissipation of these negative excess pore pressures during consolidation, considering an impermeable lining, occurs with an expansion of the ground volume which, in turn, is responsible for the swelling at the surface. As the ground volume increases with time, so does the water content around the tunnel section and, consequently, so do the axial loads acting on the lining. Since this is not a uniform swelling, bending moments on the lining, which are practically null after construction, also tend to increase with time.

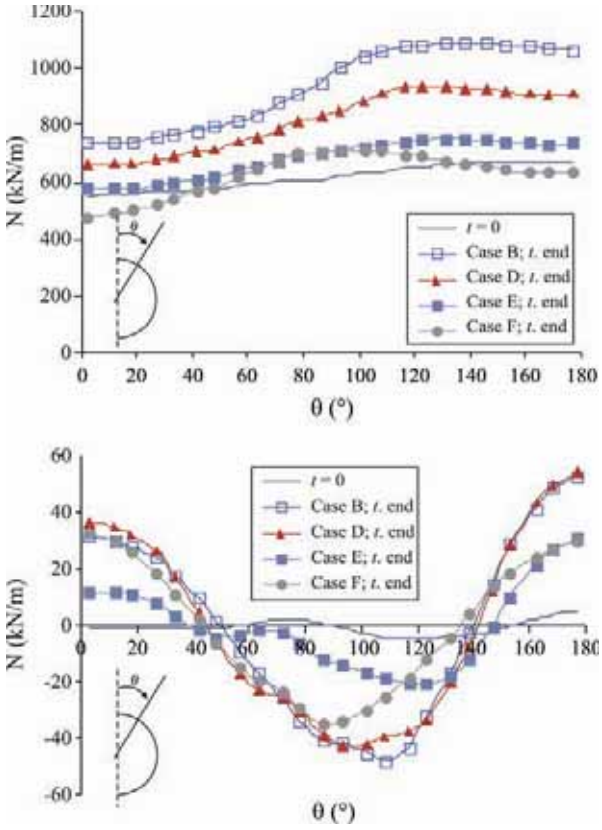

Figure 22 - Loads acting on the lining after construction (t = 0) and after consolidation (t. end): a) axial loads; b) bending moments.

A parametric study was carried out in order to clarify the influence of the construction method, by using three different relief coefficients, and the influence of the lining permeability, which was assumed permeable and with different permeability coefficients.

In what the construction method is concerned, the results show that the magnitude of the negative excess pore pressures tends to increase with the relief coefficient, since the stress variations during construction also increase. As a result, the ground movements induced by the excavation will be amplified. During consolidation, these differences tend to attenuate, particularly at the ground surface, due to the swelling derived from the water content increase around the tunnel.

The same situation occurs with axial loads on the lining, whose variations tend to reduce with time, contrary to what happens with bending moments.

The calculations carried out to analyse the influence of the soil/lining relative permeability on the time-dependent behaviour lead to an enhancement of the surface displacements with the reduction of the relative permeability. Actually, the consideration of a permeable excavation boundary assumes a groundwater flow into the filter layer located between the ground and the lining (drainage-type

tunnel), establishing a final equilibrium condition in which pore pressures are lower than the hydrostatic ones. Consequently, the effective stresses will rise more than in waterproof-type tunnels. On the other hand, the decrease of the water content on the ground surrounding the cavity leads to lower axial loads on the lining, as its permeability increases.

References

Almeida e Sousa, J. (1998) Soft Ground Tunnelling: Behaviour and Numerical Modelling. PhD Dissertation, Faculty of Science and Technology of the University of Coimbra, Coimbra, 623 pp (in Portuguese).

Atwa, M. (1996) Analyse Numérique des Écoulements d'Eau et de la Consolidation des Sols Autor des Tunnels Creusés Dans l'Argile. PhD Dissertation, Department of Géotechnique, L'École Nationale des Ponts et Chaussées, Paris, 476 pp (in French).

Drakos, I.S.; Tsotsos, S. & Hatzigogos, T. (2002) Finite element analysis for long-term settlements due to an underground excavation. Proc. of 2nd Int. Conference on Soil Structure Interaction in Urban Civil Engineering, pp. 255-262.

Ganendra, D. (1993) Finite Element Analysis of Laterally Loaded Piles. PhD Dissertation, Imperial College of Science, Technology and Medicine, London.

Lee, I.M. & Nam, S.W. (2001) The study of seepage forces acting on the tunnel lining and tunnel face in shallow tunnels. Tunnelling and Underground Space Technology v. 16:1, p. 31-40.

Lopes, M. (2004) Time-Dependent Behaviour of Shallow Tunnels. MSc Dissertation, Faculty of Engineering of the University of Porto, Porto, 217 pp, (in Portuguese).

Mair, R.J. (1979) Centrifugal Modelling of Tunnel Construction in Soft Clay. PhD Dissertation, University of Cambridge, Cambridge.

Mair, R.J. & Taylor, R.N. (1993) Prediction of clay behaviour around tunnels using plasticity solutions. Proc. of Wroth Memorial Symposium, Oxford, pp. 449-463.

New, B.M. & Bowers, K.H. (1994) Ground movement model validation at the Heathrow Express Trial Tunnel. Proc. of 7th International Symposium of Institute of Mining and Metallurgy and Brithish Tunnelling Society, London, pp. 301-329.

Schmidt, B. (1989) Consolidation settlements due to soft ground tunnelling. Proc. of 12th International Conference on Soil Mechanics and Foundation Engineering, Rio de Janeiro, v. 2, pp. 790-800.

Venda Oliveira, P. (2000) Embankments on Soft Soil – Numerical Modelling. PhD Dissertation, Faculty of Science and Technology of the University of Coimbra, Coimbra, 598 pp, (in Portuguese).

Ward, W.H. & Pender, M.J. (1981) Tunnelling in soft ground. General Report. Proc. of 10th International Conference on Soil Mechanics and Foundation Engineering, Stockholm, v. 4, pp. 261-275.

Whittle, A.J. (1990) A constitutive model for an overconsolidated clay. Sea Grant Report, MIT SG 90-15, Massachussets Institute of Technology, Cambridge.

Whittle, A.J. (1993) Evaluation of a constitutive model for overconsolidated clays. Géotecnhique, v. 43:2, p. 289-313.

Whittle, A.J.; Degroot, D.J. & Ladd, C.C. (1994) Model prediction of anisotropic behaviour of Boston Blue Clay. Journal of Geotechnical Engineering, v. 120:1, p. 199-224.

Whittle, A.J. & Kavvadas, M. (1994) Formulation of MIT-E3 model for overconsolidated clays. Journal of Geotechnical Engineering, v. 120:1, p. 173-198.

Yi, X.; Kerry Rowe, R. & Lee, K.M. (1993) Observed and calculated pore pressures and deformations induced by an earth balance shield. Canadian Geotechnical Journal, v. 30:3, pp 476-490.